Journal of Oceanography, Vol. 60, pp. 411 to 423, 2004

Tidal Mixing in the Kuril Straits and Its Impact on Ventilation in the North Pacific Ocean

TOMOHIRO NAKAMURA*, TAKAHIRO TOYODA, YOICHI ISHIKAWA and TOSHIYUKI AWAJI

Department of Geophysics, Graduate School of Science, Kyoto University, Kyoto 606-8502, Japan

(Received 19 February 2003; in revised form 30 August 2003; accepted 28 September 2003)

A numerical study using a 3-D nonhydrostatic model has been applied to baroclinic processes generated by the K_1 tidal flow in and around the Kuril Straits. The result shows that large-amplitude unsteady lee waves are generated and cause intense diapycnal mixing all along the Kuril Island Chain to levels of a maximum diapycnal diffusivity exceeding 10^3 cm^{2}s^{-1}. Significant water transformation by the vigorous mixing in shallow regions produces the distinct density and potential vorticity (PV) fronts along the Island Chain. The pinched-off eddies that arise and move away from the fronts have the ability to transport a large amount of mixed water (~14 Sv) to the offshore regions, roughly half being directed to the North Pacific. These features are consistent with recent satellite imagery and in-situ observations, suggesting that diapycnal mixing within the vicinity of the Kuril Islands has a greater impact than was previously supposed on the Okhotsk Sea and the North Pacific. To examine this influence of tidal processes at the Kurils on circulations in the neighboring two basins, another numerical experiment was conducted using an ocean general circulation model with inclusion of tidal mixing along the islands, which gives a better representation of the Okhotsk Sea Mode Water than in the case without the tidal mixing. This is mainly attributed to the added effect of a significant upward salt flux into the surface layer due to tidal mixing in the Kuril Straits, which is subsequently transported to the interior region of the Okhotsk Sea. With a saline flux into the surface layer, cooling in winter in the northern part of the Okhotsk Sea can produce heavier water and thus enhance subduction, which is capable of reproducing a realistic Okhotsk Sea Mode Water. The associated low PV flux from the Kuril Straits to the open North Pacific excites the 2nd baroclinic-mode Kelvin and Rossby waves in addition to the 1st mode. Interestingly, the meridional overturning in the North Pacific is strengthened as a result of the dynamical adjustment caused by these waves, leading to a more realistic reproduction of the North Pacific Intermediate Water (NPIW) than in the case without tidal mixing. Accordingly, the joint effect of tidally-induced transport and transformation dominating in the Kuril Straits and subsequent eddy-transport is considered to play an important role in the ventilation of both the Okhotsk Sea and the North Pacific Ocean.

Keywords:
· Tidal mixing,
· ventilation,
· eddy transport,
· Okhotsk Sea,
· North Pacific Ocean.

1. Introduction

The ventilation taking place in the North Pacific subarctic gyre reaches down to the 27.4σ_θ density layer, and its influence extends to the subtropics (e.g., Watanabe *et al*., 1994; Fine *et al*., 2001). One product of this ventilation is the North Pacific Intermediate Water (NPIW), which is characterized by a salinity minimum around 26.8σ_θ and spreads out over most of the subtropical gyre (Talley, 1993). Accordingly, the ventilation in the subarctic region may largely affect the subsurface circulation, particularly at mid-depth, in both the subarctic and subtropic gyres of the North Pacific. Since the ventilation process also creates a body of water capable of storing large amounts of greenhouse gases, such as CO_2 (Tsunogai *et al*., 1993; Yamanaka and Tajika, 1996), its study is basic to our understanding of the potential response of the ocean to increased greenhouse effects.

* Corresponding author. E-mail: nakamura@kugi.kyoto-u.ac.jp

A prominent feature of the subarctic region of the North Pacific is a shallow, strong halocline around $26.6\sigma_\theta$ due to a combination of upward Ekman pumping and a positive freshwater flux (e.g., Ohtani, 1989; Miura *et al*., 2002). Although the low salinity water in the upper part of the NPIW is thought to originate from the subarctic mixed-layer water above this halocline (e.g., Talley *et al*., 1995), the freshwater supply to the lower part of the NPIW requires a mechanism to drive the downward transfer across the strong halocline. Previous studies have identified subduction in the Okhotsk Sea and vertical diffusion in the Gulf of Alaska as likely candidate driving mechanisms. Recent field observations (Talley, 1991; Yasuda, 1997; Kono, 1998; Watanabe and Wakatsuchi, 1998) have underlined the importance of the subduction associated with sea ice formation in the Okhotsk Sea, forming the heavy Dense Shelf Water (DSW) (Kitani, 1973; Alfultis and Martin, 1987; Martin *et al*., 1998; Gladyshev *et al*., 2000). The mixing of DSW with the surroundings can produce a low potential vorticity water centered at $26.8\sigma_\theta$ (the Okhotsk Sea Mode Water, OSMW, Yasuda, 1997). This feature is favorable for the realistic production of the NPIW and is regarded as the most likely origin of the NPIW.

However, it is difficult to explain the ventilation of the lower part of the NPIW (say, below $27.0\sigma_\theta$) in terms of the above processes. This is because the direct sinking of surface water in the Okhotsk Sea influences the $27.0\sigma_\theta$ level at most (Gladyshev *et al*., 2000). In addition, vertical diffusion in the Alaskan Gyre extends only to $26.8\sigma_\theta$ (Van Scoy *et al*., 1991; You *et al*., 2000). Regarding the cabbeling effect, though it is inevitable in mixing processes of the subarctic and subtropical waters, the density increase of the mixture is less than $0.02\sigma_\theta$ below the $27.0\sigma_\theta$ density layer (Talley and Yun, 2001). These facts imply that there should be other processes causing ventilation in the lower part of the intermediate layer.

One possible mechanism for this process is vertical mixing in the Kuril Straits, which connect the Okhotsk Sea and the North Pacific. The analysis of observed chlorofluorocarbons (CFCs) concentrations indicates that the Okhotsk Sea is an important location for the ventilation of the intermediate water (Warner *et al*., 1996) and that diapycnal mixing is necessary for the formation of the Okhotsk Sea water below the $27.2\sigma_\theta$ level (Wong *et al*., 1998). Many observations have revealed the presence of vertically mixed water in the Kuril Straits and have shown that the influence of the mixing extends to 2200 m depth or more (Yasuoka, 1968; Kitani, 1973; Kawasaki and Kono, 1994; Gladyshev, 1995; Kawasaki, 1996; Freeland *et al*., 1998; Aramaki *et al*., 2001).

Recent detailed studies on the process in the Kuril Straits have suggested that the tides, especially the K_1 tide, are mainly responsible for the vertical mixing described above. In fact, the diurnal tidal currents are dominant in and around the Kuril Straits, and their speeds reach a few ms^{-1} over shallow sills and 0.3 ms^{-1} even in deep regions (Thomson *et al*., 1997; Ohshima *et al*., 2002). Such strong tidal currents are likely to cause intense vertical mixing due to interactions with the topographic features in the Kuril Straits. Modelling and theoretical studies of the tidal process have revealed that: (1) since the K_1 tide is subinertial in the Kurils, it generates topographically trapped waves; (2) these waves are amplified while circulating around the islands and produce a significant water exchange through the Kuril Straits; and (3) as the amplified currents flow over sills in the straits, large-amplitude unsteady lee waves are generated, eventually leading to enhanced diapycnal mixing due to wave breaking (Nakamura *et al*., 2000a, b; Nakamura and Awaji, 2001, 2003).

Such vigorous mixing takes place at the exit of the OSMW to the North Pacific and the entrance of the North Pacific water, which is in turn the main source of the Okhotsk Sea water. It could thus affect the water properties of the neighboring two basins. From a dynamical view point, the vertical mixing implies the supply of potential vorticity (PV) from the lateral boundary (i.e., the Kuril Island Chain) to both the North Pacific and the Okhotsk Sea. According to the ventilated thermocline theory (Pedlosky, 1996), the subsurface information travels roughly along the Sverdrup flow, thus propagating northward in a region of upward Ekman pumping and progressing eastward in the southern part of the subarctic gyre in the North Pacific. Since the Kuril Straits is located in the area corresponding to the south of the Okhotsk Sea and to the west of the North Pacific subarctic gyre, respectively, the PV flux from the Kurils could affect the circulations in the Okhotsk Sea and the subarctic gyre of the North Pacific. Moreover, since the layer of the NPIW density range corresponds to the pool zone (Huang and Russell, 1994), in which the circulation is determined by the PV flux from the western boundary region, it may be possible that the PV flux from the Kurils affects the circulation of the NPIW.

A clarification of the tidal processes and their effect on the water mass structures and the circulation in both the Okhotsk Sea and the North Pacific is therefore a key to a better understanding of the ventilation of these two basins. Moreover, examination of the thermohaline adjustment to such mixing in the western boundary region may contribute to progress in the ventilated thermocline theory.

In this paper we therefore investigate the water transformation and transport processes associated with the K_1 tide around the Kuril Straits, using a 3-dimensional nonhydrostatic model (Section 2). The impacts of the tidal mixing at the Kuril Straits on the basin scale phenomena

are then examined in Section 3 using an ocean general circulation model (OGCM). The results are summarized in Section 4.

2. Tidal Mixing in the Kuril Straits

2.1 Model and experimental design

In order to simulate baroclinic processes induced by the tides and the associated vertical mixing in and around the Kuril Straits, we use a three-dimensional nonhydrostatic model, which has been constructed on the basis of the work of Tanaka and Akitomo (2001). As shown below, intense vertical mixing around the straits will give rise to tidal fronts and associated eddies. We thus take into account the effect of a planetary-vorticity gradient by adopting the β-plane approximation. A barotropic tidal flow is calculated separately from a barotropic tide model and is given in the advection terms which work as the main forcing. The values of the eddy diffusivities (and viscosities) are chosen from parameter-sweeping tests such that the diapycnal mixing is of the same order as those estimated in the next section.

The model topography (Fig. 1) is set up from the DBDB5 (U.S. National Geophysical Data Center). The grid sizes are about 700 m horizontally and 30 m vertically. The model domain covers most of the straits in the Kuril Island Chain so as to involve the two deep passages, the Bussol and Kruzenshterna Straits, through which the major water flows are considered to take place. In addition, the propagation of topographically trapped waves and the tidally-induced mean circulation around islands and/or sills can be reproduced. Near the open boundaries, a sponge zone is adopted to prevent artificial wave reflection, where the viscosities and the horizontal diffusivities are gradually increased. In addition, baroclinic velocity, potential temperature and salinity are gradually restored to their initial values close to the open boundaries, which, in effect, acts as an artificial buoyancy flux and thereby maintains stratification in the interior.

The initial potential temperature and salinity fields are set to be horizontally uniform using the dataset of the U.S. National Oceanographic Data Center. A summertime climatology in the Kuril Basin is used from the sea surface to 1500 m depth in order to examine the modification of the Okhotsk Sea water entering the North Pacific. Since the Kuril Basin (~3200 m depth) is shallower than the deeper parts of the Pacific in this region, the initial vertical profiles between 1500 m and 3000 m depth are gradually changed to the summertime climatology of the East Kamchatka Current Water (EKCW), which acts as the local origin of the water. The baroclinic velocity is set to zero at the beginning of the calculation.

In this experiment, we direct our attention to the K_1 tide alone since the K_1 current is the largest constituent around the Kuril Island Chain (e.g., Thomson *et al*., 1997; Nakamura *et al*., 2000a). The barotropic tide model used here is the same as that of Nakamura *et al*. (2000a). The horizontal resolution, however, is taken to be the same as in this 3-dimensional model. The basic features of the calculated barotropic field are essentially the same and

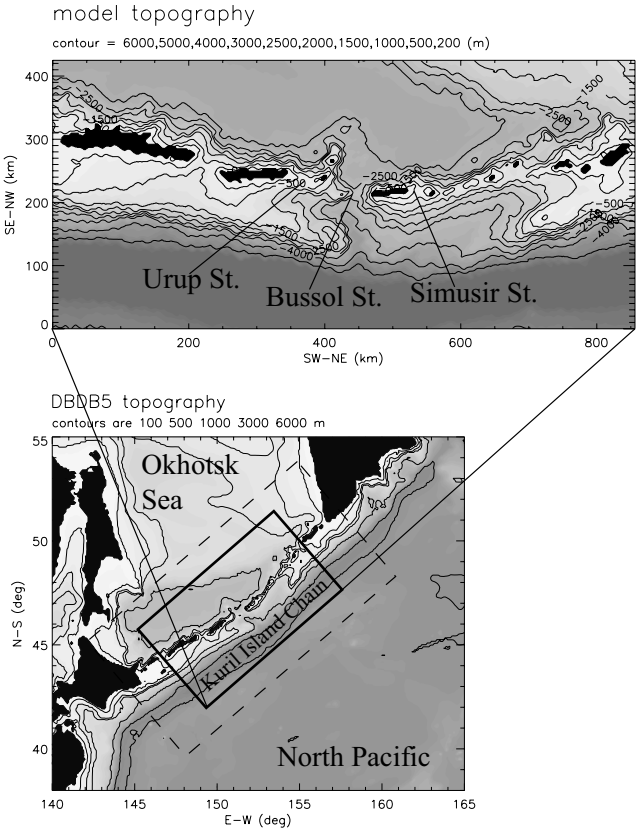

Fig. 1. Model topography of the tidal processes (upper panel). Lower panel shows the locations of the 3-D model domain (solid) and the barotropic model domain (dashed). Black colored areas indicate land grids.

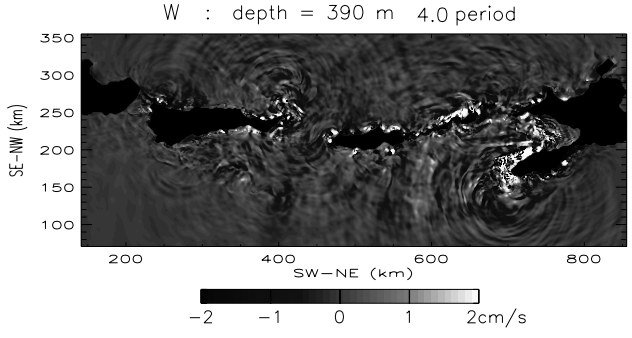

Fig. 2. Vertical velocity after 4 periods at 390 m depth.

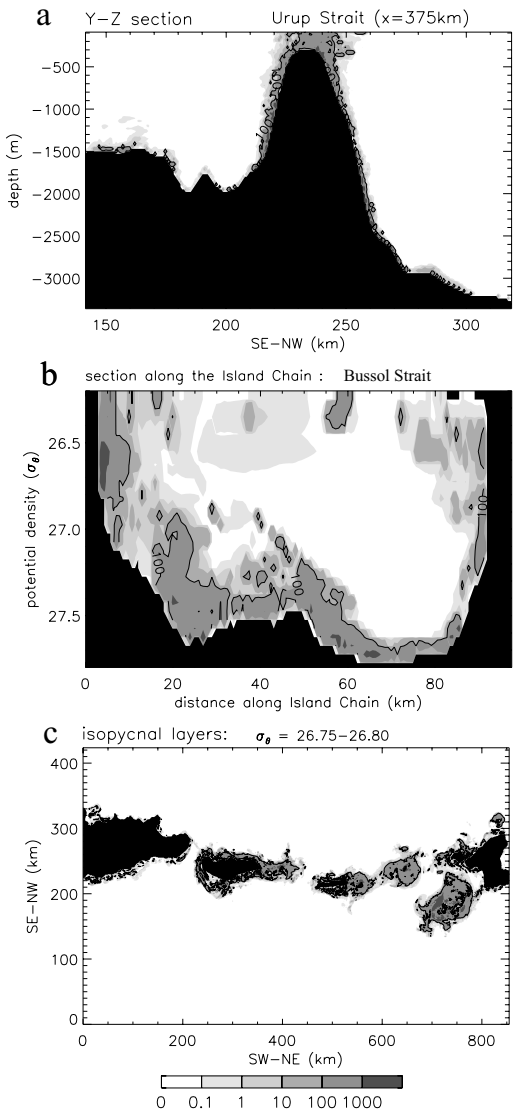

Fig. 3. Temporally averaged diapycnal diffusivity coefficients (cm^2s^{-1}) estimated from the calculated fields in the 4th period. Contour is drawn at 100 cm^2s^{-1}. (a) An example of y-z sections across the sill in the Urup Strait. (b) Bussol Strait section shown along the Island Chain, the vertical axis being potential density. (c) Horizontal distribution in the isopycnal layer of 26.75~26.8σ_θ.

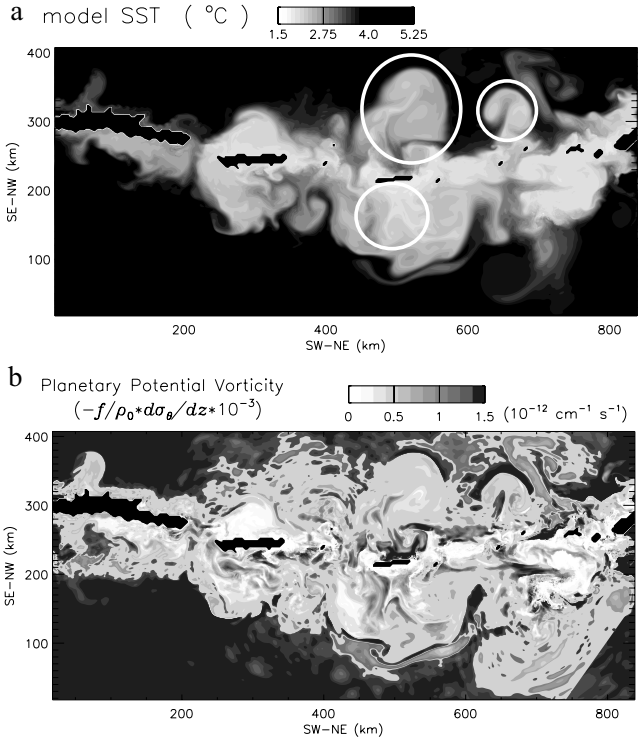

Fig. 4. (a) Potential temperature at the model sea surface (15 m depth) after 25 periods. White circles indicate eddy-like structures also seen in AVHRR thermal infrared imagery (Fig. 5). (b) Planetary part of potential vorticity after 25 periods at the model sea surface.

the harmonic constants of both tidal elevation and current field are qualitatively similar to the observed values, but an increase in horizontal resolution leads to a corresponding improvement in accuracy.

2.2 Diapycnal mixing

As in the vertical 2-dimensional case reported by Nakamura *et al*. (2000b), the main cause of mixing can be attributed to large-amplitude unsteady lee waves, which are generated around a sill top and propagate away as the flow reverses. Figure 2 shows the horizontal distribution of vertical velocity after 4 periods (after an interval of time corresponding to 4 periods) at 390 m depth, roughly corresponding to the core density layer of the NPIW. Many inertial gravity waves are present, indicating that large-amplitude unsteady lee waves are produced all along the Kuril Island Chain. Our examination of the surfaces of constant phase reveals that large-amplitude internal waves originate mainly from (1) the bank located in the northeastern Pacific region (around x = 700 km, y = 150 km), (2) the Urup Strait, and (3) sills in the northeastern part of the island chain.

To estimate the intensity of vertical mixing associated with the wave processes, we calculate diapycnal diffusivity coefficients, K_ρ, following the scaling proposed by Gregg (1989), which is based on the internal wave dynamics and observations. In doing so, due to our limited vertical grid size, a 30-m shear is used instead of the 10-m shear, so that the present calculation provides rough estimates of the diffusivity coefficients which will be discussed in Section 4 in addition to the problem concerning the application of Gregg's formula in this study. The estimated K_ρ is temporally averaged over the 4th period.

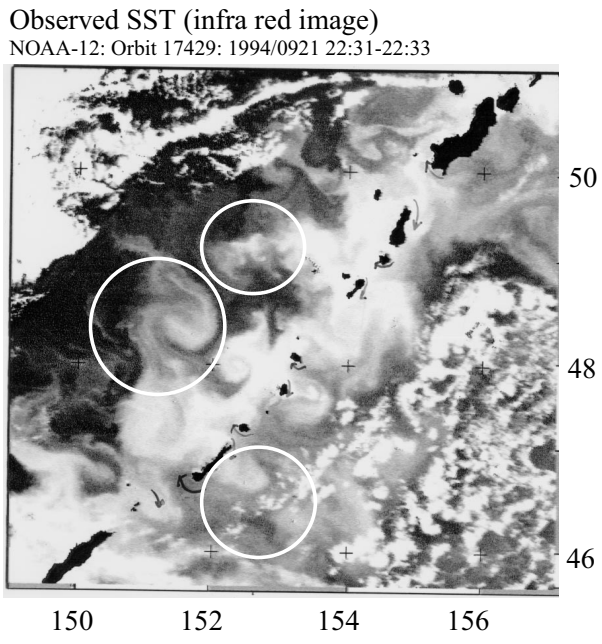

Fig. 5. AVHRR thermal infrared image of the Kuril Straits taken from the NOAA 12 satellite on September 21, 1994. White circles indicate eddy-like structures similar to features in the model SST (Fig. 4) (figure courtesy of Prof. S. Saitoh).

Figure 3(a) shows the distribution in the vertical section crossing the sill in the Urup Strait. The diapycnal diffusivity is very large over the sill, with a maximum value exceeding 1000 cm^2s^{-1}.

Figure 3(b) shows the K_ρ map across the deep Bussol Strait. On this map, σ_θ is used as a vertical axis to identify the density layers of active diapycnal mixing. Although wave-energy generation is much weaker than in the Urup Strait, considerable mixing (K_ρ > 10 cm^2s^{-1}) occurs. This result is consistent with the recently observed carbon isotopes distributions (Aramaki *et al.*, 2001). The mixing arises mainly from the clockwise transport of wave energy originating from the adjacent Urup and Simusir Straits where energetic wave generation occurs. This significant wave energy flux is attributed to the along-isobath propagation of subinertial K_1 internal tides generated over sill slopes and to the propagation of unsteady lee waves. It should be noted, then, that the density layer of the neighboring OSMW and NPIW core (~26.8σ_θ) is subject to this mixing. The outflowing Okhotsk Sea water is therefore expected to be considerably modified by tidal mixing to an extent determined by the travel time of water passing through the Strait.

The distribution of K_ρ at an isopycnal layer (26.75~26.8σ_θ) is shown in Fig. 3(c), which indicates that the above features relating to the intensity of diapycnal mixing are generally present in the Kuril Island Chain. An intense diapycnal mixing is distributed in shallow straits, around islands and over the bank, where the tidal flow is strong and thus energetic unsteady lee waves are generated. In contrast, the mixing weakens with depth (except near the bottom).

2.3 Eddy-induced offshore transport

Figure 4(a) shows the model sea surface temperature after 25 periods. The mixing with cold subsurface water produces low-temperature anomalies along the island chain, which manifest as temperature fronts and eddies. The patterns and size of eddies are generally similar to those seen in infrared imagery (Fig. 5). In particular, the eddy-like structures marked by white circles take place at almost the corresponding locations and bear such a resemblance. Such temperature fronts are known to exist almost throughout the year, although cooling in winter makes it a warm anomaly (Kitani, 1973) and their positions are quite variable. These facts strongly suggest that tidally-induced baroclinic processes are responsible for the observed fronts and eddies. It is thus reasonable to expect that diapycnal mixing induced by tidally generated unsteady lee-waves can contribute to the intense vertical mixing at the Kuril Straits.

Similarly, potential vorticity fronts are formed along the Island Chain due to the spatial variation in the strength of vertical mixing. The fronts spawn various instabilities, such as baroclinic instability and associated eddies (e.g., Pedlosky, 1987). Figure 4(b) shows a map of the planetary component of potential vorticity,

$$-\frac{f}{\rho_0}\frac{\partial \rho|_{p=0}}{\partial z}$$

(hereafter PPV), at the model sea surface after 25 periods. The tidally-induced PPV fronts evolve by the formation and release of baroclinic eddies. These eddies should contain low PPV water in their cores and thus anticyclonic eddies are easier to produce. A recent observation in the Kuril Basin clearly captured such a pinched-off eddy originating from the Kuril Straits (Itoh *et al.*, 2002).

These results indicate that eddies convey vertically well-mixed water located around the straits toward the offshore region. To quantify this transport, the volume increase of the mixed water in the deep regions is calculated (the mixed water is identified as having a PPV value either 20% lower or higher than the ambient average, and the deep region is defined here as >3000 m and/or y > 330 km). This corresponds to the offshore transport of the mixed water, assuming that diapycnal mixing is not

effective in the deep regions. The mean offshore volume flux of the mixed water during 25 periods reaches 5.7 Sv and 8.7 Sv, respectively, of which 2.6 Sv and 3.9 Sv enter the open Pacific. The volume increments are roughly constant around 25 periods, indicating that the offshore transport is roughly in a steady state and hence our estimate is meaningful. These offshore transports are attributed mainly to eddies arising and moving away from tidal fronts (at least in this model) since the net offshore transport induced by tidally-induced residual flow is about 2 Sv for the Okhotsk Sea and 1 Sv for the North Pacific (the latter is not counted in the above estimate since it takes place over a shelf break shallower than 3000 m depth).

Diapycnal mixing in the vicinity of the Kuril Islands therefore has a greater impact than was previously supposed on the Okhotsk Sea and the North Pacific as a result both of modification of in/outflowing water properties and offshore transport of the modified water associated with eddies. For example, the offshore eddy transport of the transformed water in the straits supplies significant PV and salinity fluxes to both the Okhotsk Sea and the North Pacific. The PV values of such eddies differ on average by 30–40% from the ambient water. The sea surface salinity is 0.1 psu higher than the ambient water and this difference leads to a density increase of $0.08\sigma_\theta$ in the offshore regions. Similar high sea-surface-salinity anomalies of 0.1~0.3 psu greater than the surroundings have been observed in the Kuril Straits (Reid, 1973; Gladyshev, 1995). Such fluxes will affect water masses and circulation patterns in the two basins. These aspects form the subject of the next section.

3. Impacts of Tidal Mixing on the Okhotsk Sea and North Pacific

3.1 Model and experimental design

We have performed a series of impact experiments to investigate the role of the tidal mixing at the Kuril Straits in the water mass formation and large-scale circulation in both the Okhotsk Sea and the North Pacific.

The model used is an OGCM developed at Kyoto University (Ishikawa *et al*., 2002). For a realistic reproduction of the subduction processes, this model adopts a third-order advection scheme (UTOPIA and QUICKEST; Hasumi and Suginohara (1999)) in the tracer equation. In addition, an isopycnal diffusion scheme using the eddy parameterization (Gent and McWilliams, 1990; Griffies *et al*., 1998) is incorporated together with a turbulence closure mixed layer scheme (Noh and Kim, 1999). In order to successfully simulate the subduction associated with sea ice formation in the Okhotsk Sea, a sea ice model based on the work of Ikeda (1989a, b) is added. For more adequate treatment of a free sea surface process, a σ–z hybrid vertical coordinate is adopted. The partial cell method is also used for better resolution of the bottom topography.

The model domain is nearly global (75°S–75°N). The horizontal resolution is 1° × 1° in both latitude and longitude, with 34 vertical levels spaced from 20 m near the sea surface to 400 m at the bottom. Care is taken not to smooth out the sills between the North Pacific and the Okhotsk Sea. The initial values of potential temperature and salinity are taken from the World Ocean Atlas, 1994 Monthly Data compilation (Levitus and Boyer, 1994; Levitus *et al*., 1994), to which the layers deeper than 2000 m, the northern and southern boundaries, and the exits of the Mediterranean and Red Seas are restored. The sea surface fluxes are based on the European Centre for Medium-Range Forecasts reanalysis data of a climatological seasonal variation (OMIP project; Röske (2001)) together with the so called "flux correction", except for regions around the Kuril Straits. Wind stress and heat fluxes are calculated using a model sea surface temperature based on the bulk formulae.

A 30-year spinup was performed, by which time the model ocean had reached an approximately equilibrium state. Two experiments were then conducted. In the first of these, a control situation was created by continuing the integration for another 30 years. In the second experiment, simulating the case with mixing, the vertical diffusion coefficient over the sills at the Kuril Straits was set to a constant value of 200 cm^2s^{-1}. This assumed value roughly corresponds to twice that estimated from the K_1 case alone (K_ρ of ~100 cm^2s^{-1}). The reason for this selection is that, according to the simulation experiment of tidal currents in the Kuril Straits reported by Nakamura *et al*. (2000a), the total flow speed of tidal components, except for the dominant K_1 (e.g., O_1 + P_1) in the Kuril Straits, is similar to or larger than the K_1 current speed. Taking this fact into account, we here use such a rough estimate of diapycnal diffusivity for our basic investigation of the impacts of tidal mixing on the Okhotsk Sea and the North Pacific.

The final year of the integrations (i.e., the 60th year) is used in the analysis below, except for those investigating temporal evolution after the addition of the tidal mixing.

Prior to the detailed comparison between the control and the mixing case, some discussion is needed of the quality of the OGCM itself in terms of the circulation of both the Okhotsk Sea and the North Pacific (i.e., corresponding to the control case). In general, the features of the simulated large-scale circulations in both basins are basically consistent with previous reports. For example, the large-scale cyclonic (anti-cyclonic) circulation of the Okhotsk Sea (the northwestern North Pacific) shown in Fig. 6(a) is in agreement with the observed temperature/

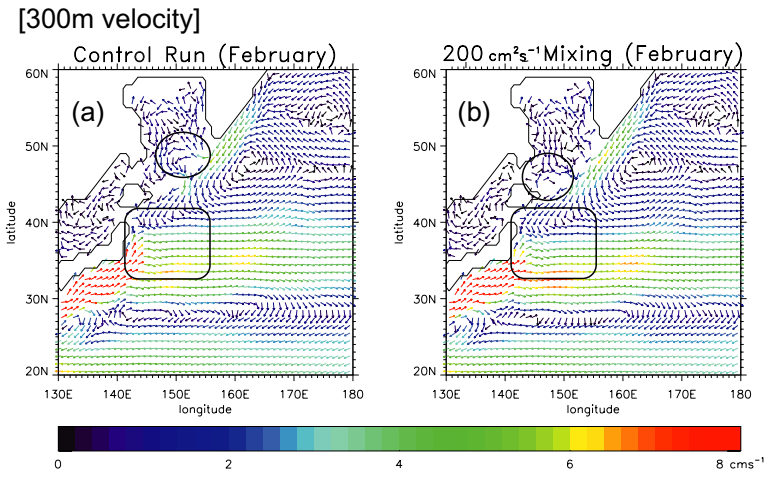

Fig. 6. Horizontal velocity vectors for (a) the control case and (b) the mixing case in the northwestern part of the North Pacific in February. See text for circles and squares in the figure.

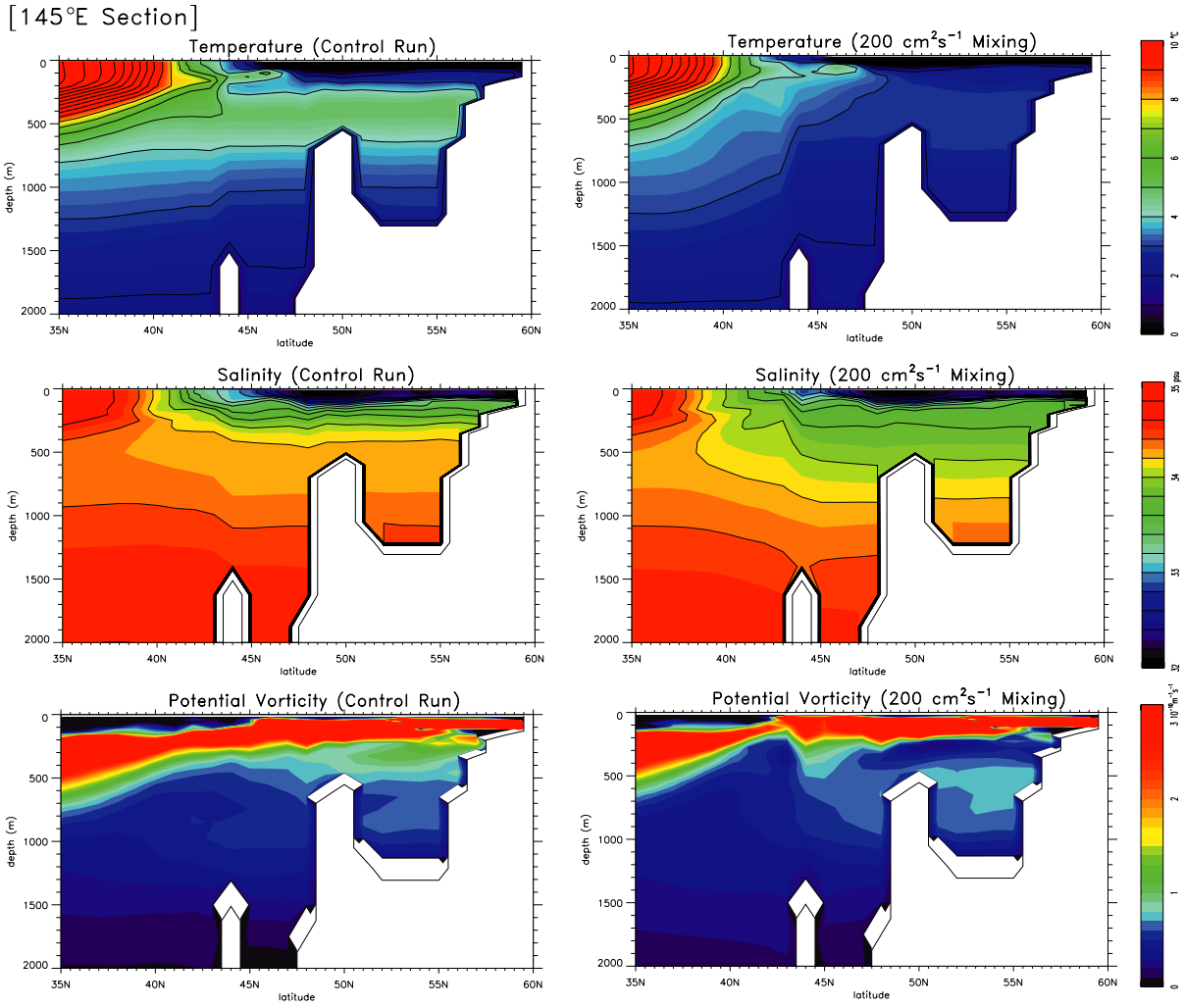

Fig. 7. Vertical section along 145°E of (top) potential temperature, (middle) salinity, and (bottom) potential vorticity for (left) the control and (right) mixing cases.

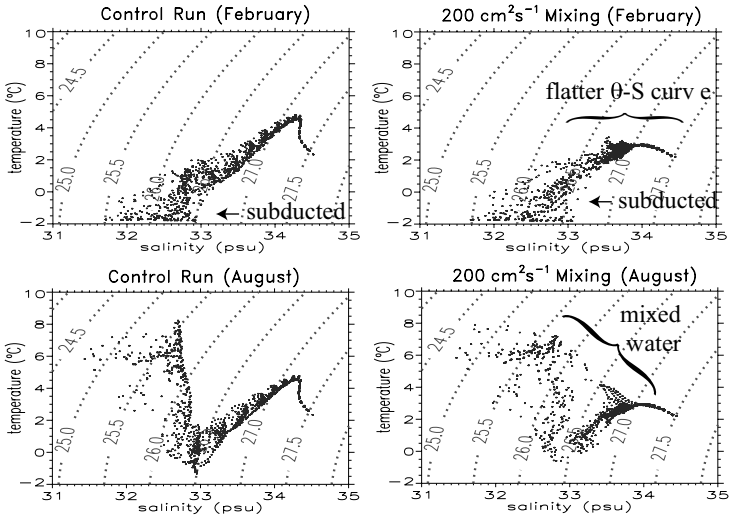

Fig. 8. θ-S diagrams in the northern part of the Okhotsk Sea in (upper) winter and (lower) summer for (left) the control and (right) mixing cases.

salinity distributions (e.g., Favorite *et al*., 1976) and a recent state estimation by data assimilation (e.g., Awaji *et al*., 2003). However, some aspects of the ocean circulation, particularly in subsurface layers, are not well presented in the control case, as discussed below.

3.2 Change in the water mass structure in the Okhotsk Sea

Figure 7 shows the results in a vertical section crossing the Okhotsk Sea to the Kuril Straits. At the Kuril Straits, fronts are produced in the mixing case in a fashion that is roughly consistent with observations. In the Okhotsk Sea, both salinity and potential temperature in the mixing case decrease in the intermediate and deep layers as compared with the control case, and approach the observed distributions. The maximum decrease exceeds 0.2 psu for salinity and 2°C for potential temperature in the intermediate layer. The latter leads to a reproduction of the observed weakening of the temperature maximum (the mesothermal water) in the Okhotsk Sea from the subarctic gyre (e.g., Kitani, 1973).

Addition of the tidal mixing also results in the lowering of PV in the intermediate layer and a much more realistic OSMW is thereby formed. As far as we are aware, this is the first successful reproduction of the OSMW by an OGCM.

To clarify the reason for the improvement in the simulation quality of the OSMW, we first examine the production of sea ice, since the DSW (the source of the OSMW) is thought to be formed by brine rejection. Both maximum volume and area of sea ice, however, are almost the same for the mixing and control cases. This is because the production rate and distribution of sea ice are mainly determined by heat and momentum fluxes at the sea surface, which are almost the same for the two cases. The amount of brine rejection is thus almost the same in both cases, although the OSMW is produced only when the tidal mixing is included.

The seasonal change in the θ-S diagram in the northern part of the Okhotsk Sea is examined next (Fig. 8). In the control case, the effect of winter cooling reaches at most the $26.5\sigma_\theta$ density layer, which means that subduction does not extend down to the intermediate layer. Thus, as seen in Fig. 7, the intermediate water in the Okhotsk Sea does not differ significantly from that in the North Pacific.

In the mixing case, diapycnally mixed water appears from the surface to the intermediate layer in summer, with a signal that is most visible in $26.5\sim26.8\sigma_\theta$ density layers. Such mixed water originates in the Kuril Straits and is transported northward by the large-scale cyclonic circulation in the Okhotsk Sea (Fig. 6). Since the vertical mixing at the Kurils induces significant upward salt flux from the saltier lower layer, the water influenced by the tidal mixing is more saline than the water that is not affected by the tidal mixing (or that in the control case).

The cooling of this more saline water in winter (together with brine rejection) enables the subduction process to involve water with density of around $26.8\sigma_\theta$, and thus the DSW density is reproduced in a much more realistic fashion. The newly formed DSW is transported to the Kuril Basin by the southward East Sakhalin Current (Fig. 6). Subsequent isopycnal mixing of the DSW with the surroundings cools an intermediate water that does not outcrop and leads to the formation of a more realistic OSMW. The subducted water is carried further downward

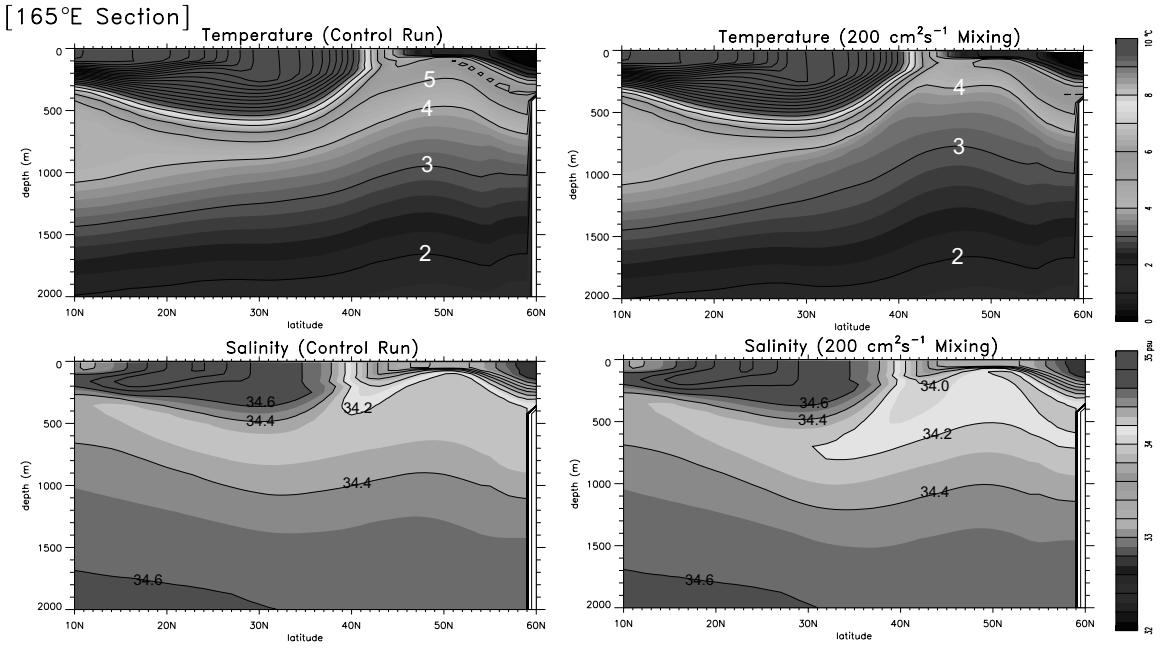

Fig. 9. Vertical section along 165°E of (upper) potential temperature and (lower) salinity for (left) the control and (right) mixing cases.

by the tidal mixing and, as a result, the rather flat θ-S curve unique to the Okhotsk Sea water is reproduced.

The tidal mixing therefore acts on the water mass structure in the Okhotsk Sea through two important processes. The first of these involves a preconditioning of the DSW production, in which salt flux by tidal mixing from the intermediate layer to the surface layer enhances the subduction associated with sea ice formation in winter. This is important in the formation of the intermediate water, the density of which the direct subduction can reach. The other process involves the direct modification of water by diapycnal mixing (after subduction) and is dominant in the water mass modification both in the Kuril Straits and in the deep layer to which the direct subduction does not extend.

In addition, the low PV water from the Kuril Straits modifies the circulation in the Okhotsk Sea (Fig. 6). For example, a westward flow in the eastern part of the Kuril Basin (circled in Fig. 6(a)) almost vanishes in the mixing case, while the anticyclonic circulation in the Kuril Basin (circled in Fig. 6(b)) is enhanced. These features in the mixing case are qualitatively consistent with the observed temperature-salinity distributions.

3.3 Thermohaline adjustment of the intermediate layer in the North Pacific

Tidal mixing in the Kuril Straits also leads to enhancement of the ventilation taking place in the intermediate water of the North Pacific. Figure 9 shows potential temperature and salinity distributions at 165°E from the subarctic to subtropic gyres. The salinity change is largest on the 27.1σ_θ density surface and has a maximum decrease of over 0.15 psu. This freshening largely originates from the more realistic production of the OSMW. On the other hand, a significant freshening is also created in deeper layers (say, 1000~1500 m), which is due to direct tidal mixing. Such changes occur in both subarctic and subtropical gyres and lead to a better reproduction of the NPIW. In addition, since these freshening processes mainly occur in the lower part of the NPIW, where the direct ventilation in the North Pacific does not reach (except in the Japan Sea), the density of the salinity minimum increases by 0.3σ_θ. In the subarctic gyre, potential temperature in the mixing case decreases by up to 1°C and a more realistic profile is reproduced in the lower part (below 400 m) of the mesothermal water as compared with the climatology shown by Ueno and Yasuda (2000).

One reason for the improved quality of the simulation is the change in the properties of the water supplied to the North Pacific. The salinity difference between the mixing and the control case increases steadily in the intermediate and deep layers on the Pacific side of the Bussol Strait after the addition of the tidal mixing (Fig. 10). A similar change is also seen on density surfaces since this is accompanied by a temperature decrease. The fresh-

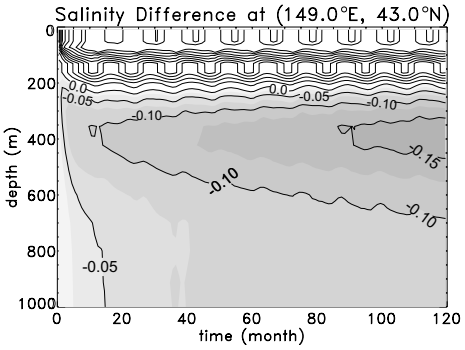

Fig. 10. Difference of salinity between the control and mixing cases on the Pacific side of the Bussol Strait after the addition of the vertical mixing.

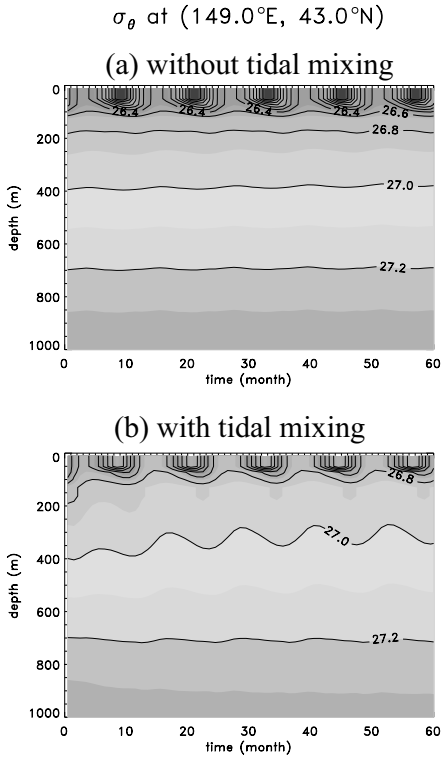

Fig. 11. Temporal evolution of density for (a) the control case and (b) the mixing case on the Pacific side of Bussol Strait after the addition of the vertical mixing.

ening is associated with the downward fresh water flux produced both by vertical mixing in the Kuril Straits and by the enhancement of the direct ventilation in the Okhotsk Sea. In addition, there is a dynamical forcing, which could change the pathways of the mixed water from the Kurils and may thus modify the water mass structure. The flux of low PV water is generated both by the direct effect of the vertical mixing given at the Kuril Straits and by the improved OSMW. Figure 11 compares the temporal evolution of density structures in the two cases on the Pacific side of the Bussol Strait after the addition of the tidal mixing. The main response is the significant change in the thickness of the intermediate layer, by which the second baroclinic mode waves are forced in addition to the first mode ones. In addition, the seasonal variation in the thickness is strong, with a maximum in spring (the PV is minimum). Such behavior is a very prominent feature of the Oyashio (e.g., Kono and Kawasaki, 1997).

The required dynamical adjustment to the PV flux arriving at the western boundary takes place through the agency of Kelvin and Rossby waves. Figure 12 shows the temporal evolution of the difference in velocity on the $27.1\sigma_\theta$ density surface after the addition of the tidal mixing. Initially, a signal travels rapidly along the coast against the Kuroshio Current, and is split into two components, one propagating along the equator and the other passing through the Indonesian Archipelago. This anomaly consists primarily of Kelvin waves. Another type of anomaly then slowly moves eastward around the boundary of the subtropic and subarctic gyres. This is associated with the second mode Rossby waves (to be precise, the higher modes are included as well). Propagation of the higher mode Rossby waves is affected by the mean flow field, so that the waves are forced to move eastward in such a strong eastward flow region. This feature differs from the classical thermohaline adjustment theory of the deep layer (e.g., Kawase, 1987; Goodman, 2001), which includes the role of equatorial Kelvin waves alone in the eastward spreading.

The propagation of both types of waves significantly modifies the circulation of the North Pacific intermediate layer. Firstly, the Kelvin waves affect the overturning conveyed through the western boundary region. In particular, water mass exchange between the subarctic and subtropical gyres is enhanced as the Oyashio is strengthened and extends further south than the zero-Sverdrup transport line (enclosed in Fig. 6). These results suggest that the reproduction of a realistic Oyashio requires tidal mixing at the Kuril Straits or at least a realistic OSMW. Secondly, the second mode Rossby waves modify the circulation (and thus overturning) in the interior region. Eventually, these processes lead to enhancement of the meridional overturning by 3 Sv at the maximum (Fig. 13). Accordingly, the effect of tidal mixing in the Kuril Straits is thought to exert a significant influence on the North Pacific circulation, mainly through the strengthening of both the shallow overturning by enhanced subduction in the Okhotsk Sea and the deep overturning by diapycnal transport of the tidally mixed water. The dynamical responses of the North Pacific, in turn, affect the pathways of the freshened water supplied from the Kuril Straits.

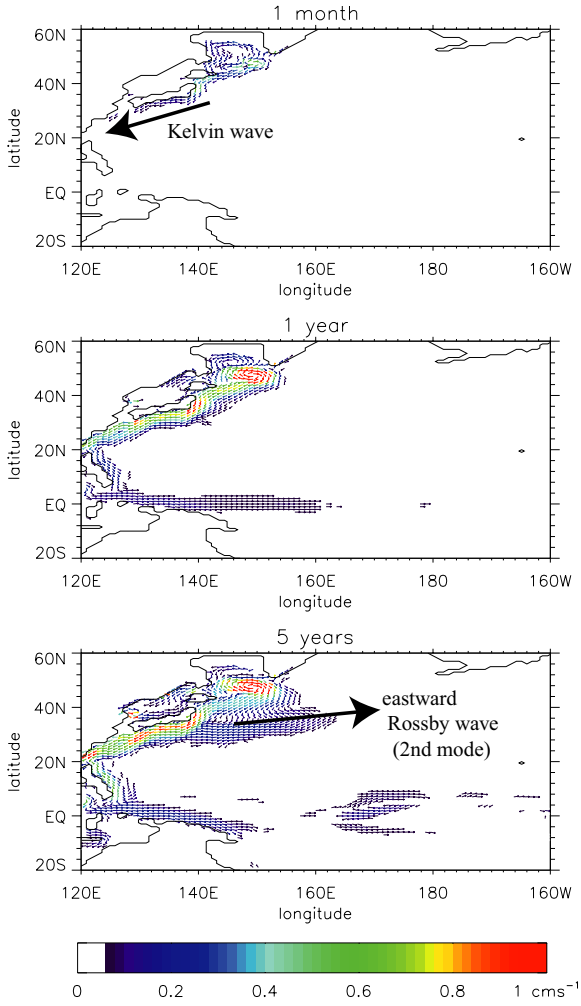

Fig. 12. Temporal evolution of velocity difference between the control and mixing cases on the density layer of 27.1σ_θ.

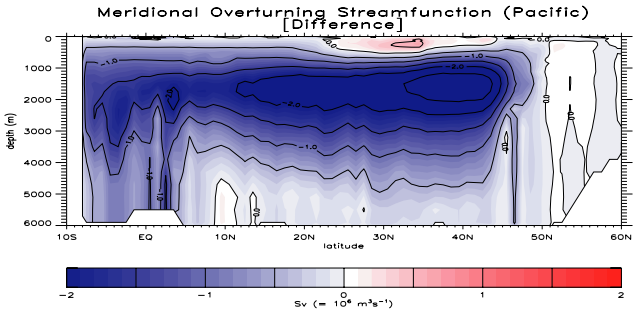

Fig. 13. Difference of the meridional overturning stream function in the North Pacific between the control and mixing cases. The values are averaged annually.

4. Summary and Discussion

Baroclinic processes generated by the K_1 tidal flow in the Kuril Straits have been investigated numerically using a 3-D nonhydrostatic model. The results revealed the generation of large-amplitude unsteady lee waves around sill tops all along the Kuril Island Chain. These waves cause intense diapycnal mixing over the shallow topographic features and near the bottom and eventually lead to a maximum diapycnal diffusivity of over 10^3 cm^2s^{-1}. Vigorous mixing in shallow regions produces low PV water. Accordingly, PV fronts are formed along the island chain, which sustain instabilities and in turn release baroclinic eddies with low core PV values. The amount of eddy-driven offshore transport away from the islands reaches 14 Sv, roughly half being directed to the North Pacific. This spreads the effect of the diapycnal mixing that occurs in the straits over wider areas of the North Pacific and the Okhotsk Sea.

To investigate the effect of such tidal processes on the Okhotsk Sea and North Pacific, we next performed numerical experiments with and without tidal mixing at the Kuril Straits using an ocean general circulation model. The results show that tidal mixing enables us to reproduce a realistic Okhotsk Sea Mode Water through the combined effects of winter cooling and saline flux penetration into the upper layer, which acts to deepen the sinking of surface water in the Okhotsk Sea. In addition, the water mass modification by tidal mixing in the Kuril Straits leads to indirect ventilation of deeper layers, as suggested by Talley (1993). As a result of these effects, the intermediate water supplied to the North Pacific becomes colder and fresher. Moreover, its PV values are lowered, which results in a strengthening of the meridional overturning in the North Pacific by up to 3 Sv. This change in the circulation pattern is caused by the dynamical adjustment effected by both the 2nd mode Kelvin and Rossby waves in addition to the first mode. The Kelvin waves are not considered in the ventilated thermocline theory, while the effect of the eastward Rossby waves is not included in the classical treatment of thermohaline adjustment of the deep layer. These modifications eventually lead to the formation of a more realistic North Pacific Intermediate Water (NPIW) for the case including tidal mixing as compared with the case without tidal mixing. In particular, the density of the corresponding salinity minimum and salinity values of the water below becomes more realistic than in the simulations using the state-of-the-art OGCMs.

Although these results have revealed the importance of the tidal mixing process in the ventilation of the North Pacific, further studies aimed at a quantitative understanding are required to clarify water transformation and transport processes around the Kuril Straits when feedback processes from wind-driven and thermohaline circulation to tidal process are included. In addition, a precise estimate of diapycnal mixing must await future intensive observations and/or improvements of the mixing

parameterization. The state-of-the-art scalings, such as that proposed by Gregg (1989), are not very suitable in a region where highly energetic wave processes occur, such as continental shelves. Nevertheless its estimate is thought to be much better than estimates calculated on the basis of the Fickian formulation (i.e., $K_z = \overline{\rho' w'} / (\partial \overline{\rho} / \partial z)$ where $\overline{(\,)}$ and $'$ denote a temporal average over one tidal period and its deviation, respectively). The Fickian-based estimation often adopted in current OGCMs tends to provide larger values of diffusivity than expected (in this case it yields values nearly one order of magnitude greater than the present estimate). Future studies are also necessary to understand the ventilation process of the North Pacific. For example, observations gathered during the Subarctic Gyre Experiment (SAGE) project revealed that the transport of subarctic water into the intermediate layer of the Mixed Water Region is often associated with small-scale eddies, the effects of which are not sufficiently incorporated in this impact experiment. Consideration of these factors is beyond the scope of the present study.

Acknowledgements

We wish to acknowledge Dr. J. P. Matthews for his critical reading and Prof. S. Saitoh (Hokkaido University, Japan) for the kind offer of NOAA 12 AVHRR imagery. We also thank anonymous reviewers for their useful comments. The authors were supported by the Subarctic Gyre Experiment (SAGE) project and by the Category 7 of MEXT RR2002 Project for Sustainable Coexistence of Human, Nature and the Earth. T.N. is also supported by the JSPS Research Fellowships for Young Scientists. Numerical Calculations were done on the VPP800 at the Data Processing Center of Kyoto University.

References

Alfultis, M. A. and S. Martin (1987): Satellite passive microwave studies of the Sea of Okhotsk Sea ice cover and its relation to oceanic processes. *J. Geophys. Res.*, **92**, 13,013–13,028.

Aramaki, T., S. Watanabe, T. Kuji and M. Wakatsuchi (2001): The Okhotsk-Pacific seawater exchange in the viewpoint of vertical profiles of radiocarbon around the Bussol' Strait. *Geophys. Res. Lett.*, **28**, 3971–3974.

Awaji, T., S. Masuda, Y. Ishikawa, N. Sugiura, T. Toyoda and T. Nakamura (2003): State estimation of the North Pacific Ocean by a four-dimensional variational data assimilation. *J. Oceanogr.*, **59**, 931–943.

Favorite, F., A. J. Dodimead and K. Nasu (1976): Oceanography of the Subarctic Pacific region, 1960–1971. *Bull. Int. North Pac. Fish. Comm.*, **33**, 187 pp.

Fine, R. A., K. A. Maillet, K. F. Sullivan and D. Willey (2001): Circulation and ventilation flux of the Pacific Ocean. *J. Geophsy. Res.*, **106**, 22,159–22,178.

Freeland, H. J., A. S. Bychkov, F. Whitney, C. Taylor, C. S. Wong and G. I. Yurasov (1998): WOCE section P1W in the Sea of Okhotsk 1. Oceanographic data description. *J. Geophsy. Res.*, **103**, 15,613–15,623.

Gent, P. R. and J. C. McWilliams (1990): Isopycnal mixing in ocean circulation models. *J. Phys. Oceanogr.*, **20**, 150–155.

Gladyshev, S. V. (1995): Fronts in the Kuril Island region. *Oceanology*, English translation, **34**, 452–459.

Gladyshev, S., S. Martin, S. Riser and A. Figurkin (2000): Dense water production on the northern Okhotsk shelves: Comparison of ship-based spring–summer observations for 1996 and 1997 with satellite observations. *J. Geophys. Res.*, **105**, 26,281–26,299.

Goodman, P. J. (2001): Thermohaline adjustment and advection in an OGCM. *J. Phys. Oceanogr.*, **31**, 1477–1497.

Gregg, M. C. (1989): Scaling turbulent dissipation in the thermocline. *J. Geophys. Res.*, **94**, 9686–9698.

Griffies, S. M., A. Gnanadesikan, R. C. Pacanowski, V. D. Larichev, J. K. Dukowicz and R. D. Smith (1998): Isoneutral diffusion in a z-coordinate ocean model. *J. Phys. Oceanogr.*, **28**, 805–830.

Hasumi, H. and N. Suginohara (1999): Sensitivity of a global ocean general circulation model to tracer advection schemes. *J. Phys. Oceanogr.*, **29**, 2730–2740.

Huang, R. X. and S. Russell (1994): Ventilation of the Subtropical North Pacific. *J. Phys. Oceanogr.*, **24**, 2589–2605.

Ikeda, M. (1989a): A coupled ice-ocean mixed layer model of the marginal ice zone to wind forcing. *J. Geophys. Res.*, **94**, 9699–9709.

Ikeda, M. (1989b): Snow cover detected by diurnal warming of sea ice/snow surface off Labrador in NOAA imagery. *IEEE Trans. Geosci. Remote Sens.*, **27**, 552–560.

Ishikawa, Y., T. Awaji, T. Toyoda and N. Komori (2002): Construction of a data assimilation system for ocean general circulations—Determination of weight parameters for the adjoint method—. *Proc. of Int. Simposium "En route to GODAE"*, **B09-21**, Biarritz, France.

Itoh, M., Y. Kawasaki, K. I. Ohshima, G. Mizuta, Y. Fukamachi and M. Wakatsuchi (2002): Anticyclonic eddies in the Okhotsk Sea. *Eos. Trans. AGU, 83(4), Ocean Sciences Meet. Suppl., Abstract*, OS11C-53.

Kawasaki, Y. (1996): The origin of the North Pacific Intermediate Water—from the observations in the Okhotsk Sea—. *Kaiyo Monthly*, **28**, 545–552 (in Japanese).

Kawasaki, Y. and T. Kono (1994): Distribution and transport of Subarctic Waters around the middle of Kuril Islands. *Umi to Sora*, **70**, 71–84 (in Japanese with English abstract and figure captions).

Kawase, M. (1987): Establishment of deep ocean circulation driven by deep-water production. *J. Phys. Oceanogr.*, **17**, 2294–2317.

Kitani, K. (1973): An oceanographic study of the Okhotsk Sea—particularly in regard to cold waters. *Bulletin of the Far Seas Fisheries Research Laboratory*, **9**, 45–77.

Kono, T. (1998): Formation of the salinity minimum in the Mixed Water Region between the Oyashio and Kuroshio Fronts. *Deep-Sea Res. I*, **45**, 2035–2057.

Kono, T. and Y. Kawasaki (1997): Result of CTD and mooring observations southeast of Hokkaido. 2, Annual variations of water mass structure and salt flux of the Oyashio. *Bull. Hokkaido Natl. Fish. Res. Inst.*, **61**, 83–95.

Levitus, S. and T. P. Boyer (1994): World Ocean Atlas 1994, Vol. 4, Temperature. *NOAA Atlas NESDIS 4*, U.S. Govt. Printing Office, Washington, D.C., 117 pp.

Levitus, S., R. Burgett and T. P. Boyer (1994): World Ocean Atlas 1994, Vol. 3, Salinity. *NOAA Atlas NESDIS 3*, U.S. Govt. Printing Office, Washington, D.C., 99 pp.

Martin, S., R. Drucker and K. Yamashita (1998): The production of ice and dense shelf water in the Okhotsk Sea polynyas. *J. Geophys. Res*., **103**, 27,771–27,782.

Miura T., T. Suga and K. Hanawa (2002): Winter mixed layer and formation of dichothermal water in the Bering Sea. *J. Oceanogr*., **58**, 815–823.

Nakamura, T. and T. Awaji (2001): A growth mechanism for topographic internal waves generated by an oscillatory flow. *J. Phys. Oceanogr*., **31**, 2511–2524.

Nakamura, T. and T. Awaji (2003): Tidally-induced diapycnal mixing in the Kuril Straits and its roles in water transformation and transport: A three dimensional nonhydrostatic model experiment. *J. Geophys. Res*. (submitted).

Nakamura, T., T. Awaji, T. Hatayama, K. Akitomo and T. Takizawa (2000a): Tidal exchange through the Kuril Straits. *J. Phys. Oceanogr*., **30**, 1622–1644.

Nakamura, T., T. Awaji, T. Hatayama, K. Akitomo, T. Takizawa, T. Kono, Y. Kawasaki and M. Fukasawa (2000b): The generation of large-amplitude unsteady lee waves by subinertial K_1 tidal flow: a possible vertical mixing mechanism in the Kuril Straits. *J. Phys. Oceanogr*., **30**, 1601–1621.

Noh, Y. and H. J. Kim (1999): Simulations of temperature and turbulence structure of the oceanic boundary layer with the improved near-surface process. *J. Geophys. Res*., **104**, 15,621–15,634.

Ohshima, K. I., M. Wakatsuchi, Y. Fukamachi and G. Mizuta (2002): Near-surface circulation and tidal currents of the Okhotsk Sea observed with the satellite-tracked drifters. *J. Geophys. Res*., **107**, art. no. 3195.

Ohtani, K. (1989): The role of the Sea of Okhotsk on the formation of the Oyashio water. *Umi to Sora*, **65**, 63–83 (in Japanese with English abstract and figure captions).

Pedlosky, J. (1987): *Geophysical Fluid Dynamics*. 2nd ed., Springer-Verlag, New York, 710 pp.

Pedlosky, J. (1996): *Ocean Circulation Theory*. Springer-Verlag, Berlin, Heidelberg, 453 pp.

Reid, J. L. (1973): *North Pacific Ocean Waters in Winter*. The Johns Hopkins Press, Baltimore, 85 pp.

Röske, F. (2001): An atlas of surface fluxes based on the ECMWF re-analysis—a climatological dataset of force global ocean general circulation models. *Max-Planck-Institut f*$\dot{u}$ *Meteorologie*, *323*, 26 pp.

Talley, L. D. (1991): An Okhotsk Sea water anomaly: implications for ventilation in the North Pacific. *Deep-Sea Res*., **38**, S171–S190.

Talley, L. D. (1993): Distribution and formation of North Pacific Intermediate Water. *J. Phys. Oceanogr*., **23**, 517–537.

Talley, L. D. and J. Y. Yun (2001): The role of cabbeling and double diffusion in setting the density of the North Pacific intermediate water salinity minimum. *J. Phys. Oceanogr*., **31**, 1538–1549.

Talley, L. D., Y. Nagata, M. Fujimura, T. Iwao, T. Kono, D. Inagake, M. Hirai and K. Okuda (1995): North Pacific Intermediate Water in the Kuroshio/Oyashio Mixed Water Region. *J. Phys. Oceanogr*., **25**, 475–501.

Tanaka, K. and K. Akitomo (2001): Baroclinic instability of density current along a sloping bottom and the associated transport process. *J. Geophys. Res*., **106**, 2621–2638.

Thomson, R. E., P. H. LeBlond and A. B. Rabinovich (1997): Oceanic odyssey of a satellite-tracked drifter: North Pacific variability delineated by a single drifter trajectory. *J. Oceanogr*., **53**, 81–87.

Tsunogai, S., T. Ono and S. Watanabe (1993): Increase in total carbonate in the western North Pacific water and a hypothesis on the missing sink of anthropogenic carbon. *J. Oceanogr*., **49**, 305–315.

Ueno, H. and I. Yasuda (2000): Distribution and formation of the mesothermal structure (temperature inversions) in the North Pacific subarctic region. *J. Geophys. Res*., **105**, 16,885–16897.

Van Scoy, K. A., D. B. Olson and R. A. Fine (1991): Ventilation of North Pacific Intermediate Waters: The role of the Alaskan Gyre. *J. Geophys. Res*., **96**, 16,801–16,810.

Warner, M. J., J. L. Bullister, D. P. Wisegraver, R. H. Gammon and R. F. Weiss (1996): Basin-wide distributions of chlorofluorocarbons CFC-11 and CFC-12 in the North Pacific. *J. Geophys. Res*., **101**, 20,525–20,542.

Watanabe, T. and M. Wakatsuchi (1998): Formation of $26.8\sigma_\theta$ water in the Kuril Basin of the Sea of Okhotsk as a possible origin of North Pacific Intermediate Water. *J. Geophys. Res*., **103**, 2849–2865.

Watanabe, Y., K. Harada and K. Ishikawa (1994): Chlorofluorocarbons in the central North Pacific and southward spreading time of North Pacific intermediate water. *J. Geophys. Res*., **99**, 25,195–25,213.

Wong, C. S., R. J. Matear, H. J. Freeland, F. A. Whitney and A. S. Bychkov (1998): WOCE line P1W in the Sea of Okhotsk 2. CFCs and the formation rate of intermediate water. *J. Geophys. Res*., **103**, 15,625–15,642.

Yamanaka, Y. and E. Tajika (1996): The role of the vertical fluxes of particulate organic matter and calcite in the oceanic carbon cycle: Studies using biogeochemical general circulation model. *Global Biogeochem. Cycles*, **10**, 361–382.

Yasuda, I. (1997): The origin of the North Pacific intermediate water. *J. Geophys. Res*., **102**, 893–910.

Yasuoka, T. (1968): Hydrography in the Okhotsk Sea-(2). *The Oceanographical Magazine*, **20**, 55–63.

You, Y., N. Suginohara, M. Fukasawa, I. Yasuda, I. Kaneko, H. Yoritaka and M. Kawamiya (2000): Roles of the Okhotsk Sea and Gulf of Alaska in forming the North Pacific Intermediate Water. *J. Geophys. Res*., **105**, 3253–3280.